ՀՀ ԿՐԹՈՒԹՅԱՆ, ԳԻՏՈՒԹՅԱՆ, ՄՇԱԿՈՒՅԹԻ ԵՎ ՍՊՈՐՏԻ
ՆԱԽԱՐԱՐՈՒԹՅՈՒՆ
ԵՐԵՎԱՆԻ ՊԵՏԱԿԱՆ ՀԱՄԱԼՍԱՐԱՆ

ԱԴԱՄՅԱՆ ԺԻՐԱՅՐ ԱՇՈՏԻ

ՑԱԾՐ ՉԱՓԱՅԻՆ ՔՎԱՆՏԱՅԻՆ ՄԱԳՆԻՍԱԿԱՆՈՒԹՅԱՆ ՈՐՈՇ ԽՆԴԻՐՆԵՐ

Ա 04.02 - «Տեսական ֆիզիկա» մասնագիտությամբ
ֆիզիկամաթեմատիկական գիտությունների թեկնածուի
գիտական աստիճանի հայցման ատենախոսության

ՍԵՂՄԱԳԻՐ

ԵՐԵՎԱՆ 2025

THE MINISTRY OF EDUCATION, SCIENCE, CULTURE AND SPORT OF RA
YEREVAN STATE UNIVERSITY

ADAMYAN ZHIRAYR

SOME PROBLEMS OF LOW DIMENSIONAL QUANTUM MAGNETISM

Thesis for the degree of Candidate of Physical and Mathematical Sciences
Speciality 01.04.02 “Theoretical Physics”

ABSTRACT

YEREVAN 2025

Ատենախոսության թեման հաստատվել է Երևանի պետական համալսարանում

Գիտական ղեկավար՝	ֆիզ.-մաթ. գիտ. թեկնածու Վ. Ռ. Օհանյան
Պաշտոնական Ընդդիմախոսներ՝	ֆիզ.-մաթ. գիտ. դոկտոր, պրոֆեսոր Ա. Ժ. Մուրադյան ֆիզ.-մաթ. գիտ. թեկնածու, պրոֆեսոր Յ. Շնակ
Առաջատար կազմակերպություն՝	Ա. Ի. Ալիխանյանի անվան ազգային գիտական լաբորատորիա (Երևանի ֆիզիկայի ինստիտուտ)

Ատենախոսության պաշտպանությունը կայանալու է 2025թ. հունիսի 2-ին ժամը 12:00-ին Երևանի պետական համալսարանում գործող Ֆիզիկայի 049 Մասնագիտական խորհրդի նիստում:

Հասցե՝ 0025 Երևան, Ալեք Մանուկյան փ. 1, ԵՊՀ

Ատենախոսությանը կարելի է ծանոթանալ ԵՊՀ գրադարանում:

Սեղմագիրն առաքված է 2025թ. մայիսի 2-ին:

Մասնագիտական խորհրդի գիտական քարտուղար՝		Դոցենտ Վ. Պ. Քալանթարյան

The thesis theme is approved at the Yerevan State University

Scientific Supervisor:	Candidate of Phys. Math. Sciences,	V. R. Ohanyan
Official Opponents:	Doctor of Phys. Math. Sciences, Prof.	A. Zh. Muradyan
	Doctor of Philosophy, Prof.	J. Schnack
Leading Organization:	A. I. Alikhanyan National Science Laboratory (Yerevan Physics Institute)	

The defence of the thesis will take place at 12:00 on June 2, 2025, during the session of the Specialized Council 049 of Physics at the Yerevan State University.

Address: 1 Alex Manoogian Street, 0025 Yerevan, Armenia.

The thesis is available in the Yerevan State University library.

The abstract was distributed on 2 May, 2025.

Scientific secretary of the Specialized Council`		Associate professor V. P. Kalantaryan

GENERAL DESCRIPTION OF THE WORK

Relevance of the topic. Lattice spin models lie at the most fundamental microscopic description of the physical properties of magnetic materials. They are the models of localized magnetic moments (spins), interacting with each other by a special kind of quantum interaction, the exchange interaction. Interacting spin models with only a few (non-macroscopic) particles, which sometimes are referred to as 0-dimensional, can be separated from the general many-body models. The finite spin clusters are realized in nature by a special class of magnetic materials, known as single-molecule magnets (SMMs). The corresponding materials are molecular crystals with transitional metal ions within the chemical structure of molecules.

Quantum entanglement, being one of the fundamental concepts of quantum physics, lies at the basis of the physics behind the quantum technologies (in the basis of quantum computations, communication, teleportation, and information processing). In addition, entanglement enables research advantages in the study of quantum phase transitions and collective phenomena in many-body systems and condensed matter physics. Quantum spin models have been extensively investigated in the context of quantum information processing due to the possibility of creating and manipulating quantum entanglement between particular spins of the system, which carry the properties of qubits.

In the present thesis, several Heisenberg spin models are considered. Their quantum and thermal entanglement features and the dependence of the entanglement measure, negativity, on various physical parameters are studied. Particularly, the effects of Landé g-factors, as well as temperature, external magnetic field, and exchange interaction constants, are examined. The main goal of the present research is to figure out how non-conserving magnetization affects entanglement measures like negativity.

The problem of creating entangled states for certain models of molecular magnets and finding optimal parameters for controlling them using a magnetic field was also considered. The relevance of the present thesis is based on the constructing SMM models and considering them as objects of quantum technologies.

The aim of the thesis is to develop methods for enhancing and controlling the entanglement in several models of molecular magnets. Particularly, the following issues have been addressed in the thesis:

1. Spin-1/2 completely anisotropic XYZ and XXZ mixed spin-(1/2,1) dimers with two different but isotropic Landé g-factors were studied. The problem of optimization and manipulation of quantum entanglement was theoretically solved.

2. The control and optimization problem of quantum entanglement in triangular-shaped Mixed spin-$(1/2, 1/2, 1)$ molecular magnet model by means of the magnetic field when g-factors of spins are non-uniform was considered.

3. Basic quantum characteristics of the mixed spin-$(1/2, 1, 1/2)$ Heisenberg trimer designed for theoretical modeling of molecular nanomagnets such as the heterotrinuclear coordination compound $Cu^{II}Ni^{II}Cu^{II}$ in the presence of the external magnetic field was investigated. Distributions of entanglement, and the l_1-norm of quantum coherence under the influence of an external magnetic field have been examined.

4. Thermal, bipartite, and tripartite entanglements in mixed spin-$(1/2, 1, 1/2)$ and mixed spin $(1/2, 1/2, 1)$ trimers have also been investigated.

Scientific novelty.

The scientific novelty of this work lies in its comprehensive and analytically rigorous investigation of quantum entanglement in low-dimensional magnetic systems featuring non-conserving magnetization. The study focuses on Heisenberg spin dimers and trimers with differing Landé g-factors and exchange couplings. Thus, the main tool of enhancement and manipulation of the entanglement is non-conserved magnetization or the magnetization operator, which does not commute with the Hamiltonian. Non-conserving magnetization results in significant changes in the magneto-thermal properties of the model. The most prominent difference can be observed in the zero temperature magnetization curves, where the magnetization's continuous dependence on the magnetic field can be seen within the same eigenstate. Even minimal inhomogeneity in g-factors can dramatically enhance entanglement. Furthermore, the work bridges theoretical modeling with experimental relevance by analyzing systems that correspond to real molecular nanomagnets, thereby proposing practical strategies for magnetic control of quantum entanglement. This paves the way for applications in quantum information processing, particularly in the design of spin-based qubits

and quantum memory units based on single-molecule magnets.

Practical importance. Single molecular magnets (SMMs) have demonstrated significant potential as building blocks for quantum technologies due to their inherent scalability, tunability, and long coherence times. The unique properties exhibited by SMMs have led to their integration into hybrid devices, emphasizing their quantum nature. By leveraging this approach, spintronic molecular devices enable the manipulation and reading of spin states, facilitating the implementation of quantum algorithms.

SMMs possess long coherence times, a crucial aspect for their application in quantum technologies. These extended coherence times allow for the execution of logical operations without information loss before the completion of the process. Magnetic molecules collect all the essential attributes required for qubits, namely:

- Well-defined states
- Long coherence times
- Initialization of the system in well-defined states
- Entanglement and/or superposition of states
- Read-out of the quantum states

They have been proposed as electron spin qubits due to the ease with which electronic spins can be manipulated via external stimuli such as temperature, magnetic fields, or electromagnetic pulses. The ability to chemically modify magnetic molecules' structural and electronic characteristics enables the proximity of two or more units with desired properties. This feature is crucial for constructing quantum gates necessary for implementing quantum operations. SMMs with switchable linker between units have been proposed for quantum simulations, as exemplified theoretically by Cr_7Ni dimers modeling quantum gates.

The basic results to be defended are as follows:

1. In the mixed-spin dimer effects of any system parameter can be countered by applying an appropriate magnetic field, which allows us to achieve the maximum possible entanglement.

2. In antiferromagnetic dimers, increasing the magnetic field reduces entanglement. In contrast, ferromagnetic systems exhibit more complex behavior: when g_1 is positive, certain negative values of g_2 cause the system to transition into a state with greater entanglement. This reveals a significant property: entangled states can be realized in spin systems with purely ferromagnetic interactions between particles.

3. The most significant impact of non-conserved magnetization was observed in situations with uniform antiferromagnetic couplings (where $J_1 = J_2 > 0$) triangle system, leading to a substantial increase in Ne_{23}. This effect is robust; even small variations($g_2 > g_1$) between g_2 and g_1 result in a value of $Ne_{23}^3 \simeq 6.7 Ne_{23}^{(3+9)_0} \simeq 0.47$, which is just six percent less than the maximal possible value of negativity.

4. Three entanglement regimes (fully separable, biseparable, tripartite entangled) controllable by a magnetic field is possible. For $J_1 = J_2 > 0$, these regimes are only possible when $g_2 > g_1$, when magnetization is non-conserving.

5. For systems with non-uniform g-factors, the temperature range in which negativity remains significantly non-zero is similar to that of uniform g-factor systems. However, a temperature range with substantially higher entanglement emerges. High negativity between particles 1 and 3 persists almost until T/J = 0.2. Furthermore, in the case of ferromagnetic coupling constants that are characterized by the complete absence of entangled states at positive g-factors, introducing negative g-factors creates entangled states at absolute zero and significantly extends the temperature range where negativity differs from zero.

6. $Cu^{2+}Ni^{2+}Cu^{2+}$ molecular complex exhibits significant bipartite entanglement between the Cu^{2+} and Ni^{2+} magnetic ions, as well as considerable tripartite entanglement among all three constituent Cu^{2+} and Ni^{2+} magnetic ions. This entanglement persists at relatively high temperatures (up to 37 K) and strong magnetic fields (up to 46 T). In contrast, the bipartite entanglement between the two outer Cu^{2+} magnetic ions occurs only in moderate magnetic fields (ranging from 23 T to 46 T) and disappears at a much lower threshold temperature (approximately 14 K).

7. The molecular compound offers an intriguing quantum resource, particularly when examining the star-shaped state that emerges within the singlet state at low magnetic fields ($B \leq 23T$) and the W-like state found within the triplet state at moderately strong magnetic fields ($23T < B < 46T$). Additionally, we have theoretically predicted that the molecular nanomagnet exhibits a high degree of quantum coherence, which persists even at elevated temperatures despite significant thermal fluctuations.

Approbation of the work. The results of the thesis were reported at the conferences "The XIX International Conference on Symmetry Methods in Physics" (Yerevan, 2024), "88th Annual Meeting of the DPG and DPG Spring Meeting" (Regensburg, Germany, 2025) and have been discussed at the seminars of the Chair of Theoretical Physics of Yerevan State University

Publications. Four papers were published on the topic of the thesis.

Structure of the thesis. The thesis consists of an Introduction, three Chapters, a Conclusion and a bibliography. It contains 123 pages, including 38 figures.

CONTENT OF THE THESIS

In the **Introduction**, the topic's relevance and motivation are discussed. Several general statements are clarified, and key quantities are defined.

In **Chapter 1** the spin-1/2 Heisenberg dimer, the mixed spin-(1/2,1) Heisenberg dimer and their quantum entanglement were considered; particularly, the dependence of the entanglement on the system characteristics and the external magnetic field. The quantum entanglement in this chapter is determined using two different methods, namely 'Negativity' and 'Concurrence'. The dependence of the corresponding quantities on spins Landé g-factors, system anisotropy constants and exchange constants is discussed.

For a spin-1/2 two-particle system, the Hamiltonian will have the following form:

$$H = J((1+\gamma)S_1^x S_2^x + (1-\gamma)S_1^y S_2^y + \Delta S_1^z S_2^z) + D_z(S_1^x S_2^y - S_1^y S_2^x) - B(g_1 S_1^z + g_2 S_2^z) \quad (1)$$

where $S_{1,2}^{x,y,z}$ are the components of the spin-1/2 operator, g_1 g_2 are Landé g-factors, respectively, of the first and second particles, J is the exchange interaction between particles, Δ and γ are constants of Z and XY anisotropies respectively, the magnetic field B is directed along the z axis. For the

eigenvalues and eigenfunctions of the Hamiltonian, we have the following expressions:

$$\varepsilon_{1,2} = -\frac{J\Delta}{4} \mp \frac{1}{2}\sqrt{B^2 g_-^2 + D_z^2 + J^2}, \qquad \varepsilon_{3,4} = \frac{J\Delta}{4} \mp \frac{1}{2}\sqrt{B^2 g_+^2 + J^2\gamma^2} \tag{2}$$

$$\Psi_{1,2} = \frac{1}{\sqrt{1+A_\mp^2}}(|\uparrow\downarrow\rangle + A_\mp|\downarrow\uparrow\rangle), \qquad \Psi_{3,4} = \frac{1}{\sqrt{1+B_\mp^2}}(|\uparrow\uparrow\rangle + B_\mp|\downarrow\downarrow\rangle)$$

$$A_\mp = \frac{Bg_- \mp \sqrt{B^2 g_-^2 + J^2 + D_z^2}}{\sqrt{J^2 + D_z^2}}, \qquad B_\mp = \frac{Bg_+ \mp \sqrt{B^2 g_+^2 + J^2\gamma^2}}{J\gamma}, \quad g_\pm = g_1 \pm g_2.$$

From expressions we see that at $g_- = 0$, maximally entangled states $\Psi_{1,2} = \frac{1}{\sqrt{2}}(|\uparrow\downarrow\rangle + |\downarrow\uparrow\rangle)$ are obtained and at $g_+ = 0$ the states $\Psi_{3,4} = \frac{1}{\sqrt{2}}(|\uparrow\uparrow\rangle + |\downarrow\downarrow\rangle)$. Proceeding from the fact that the eigenvalues and eigenstates of the Hamiltonian are symmetric with respect to the sign of the magnetic field, we will consider only positive fields. For antiferromagnetic interaction and positive magnetic field, the system exhibits ψ_1 and/or ψ_3 ground states. Let's consider the dependence of concurrence(C) on the magnetic field for several values of g_2. Let's fix the other parameters of the system as $\Delta = 0.5$, $D = 0.1$, $J = 5$, $g_1 = 1$, $\gamma = 0.5$(Fig.1a). Then for negative g_2, the system is in a state Ψ_1. The approximate maximum value of entanglement is reached near the point $B = 0$ and decreases with the increasing magnetic field. For positive g_2, system exhibits $\Psi_1 \mapsto \Psi_3$ transition at some critical point. The maximum is reached before the transition when $g_2 = 1$, the transition corresponds to a jump down, after which the entanglement decreases.

Let us consider another case of parameters: $\Delta = 0.5$, $D = 0.1$, $J = 5$, $g_1 = 1$, $\gamma = 2$(Fig.1b). Here, for negative g_2, the transition $\Psi_3 \mapsto \Psi_1$ takes place. The maximum is reached before it, when $g_2 = -1$. For positive g_2, the system is in a state Ψ_3. The decrease of g_2 corresponds to an increase in the entanglement.

The Hamiltonian of a two-particle system with mixed spins, have following form:

$$H = J(S_1^x\mu_2^x + S_1^y\mu_2^y + \Delta S_1^z\mu_2^z) + D(\mu^z)^2 - B(g_1 S_1^z + g_2\mu_2^z), \tag{3}$$

where $S_1^{x,y,z}$ are the components of the spin-1/2 operator and $\mu_2^{x,y,z}$ of the spin-1 operator. For eigenfunctions of the Hamiltonian, we obtain the following expressions.

$$\Psi_{1,2} = |\mp\tfrac{1}{2}, \mp 1\rangle, \quad \Psi_{3,4} = C_1^\pm|-\tfrac{1}{2}, 1\rangle \mp C_1^\mp|\tfrac{1}{2}, 0\rangle, \quad \Psi_{5,6} = C_2^\pm|\tfrac{1}{2}, -1\rangle \mp C_2^\mp|-\tfrac{1}{2}, 0\rangle, \tag{4}$$

$$C_1^\pm = \sqrt{\tfrac{1}{2}\left(1 \pm \frac{J\Delta - 2D - 2g_-B}{\sqrt{(J\Delta - 2D - 2g_-B)^2 + 8J^2}}\right)}, \quad C_2^\pm = \sqrt{\tfrac{1}{2}\left(1 \pm \frac{J\Delta - 2D + 2g_-B}{\sqrt{(J\Delta - 2D + 2g_-B)^2 + 8J^2}}\right)}$$

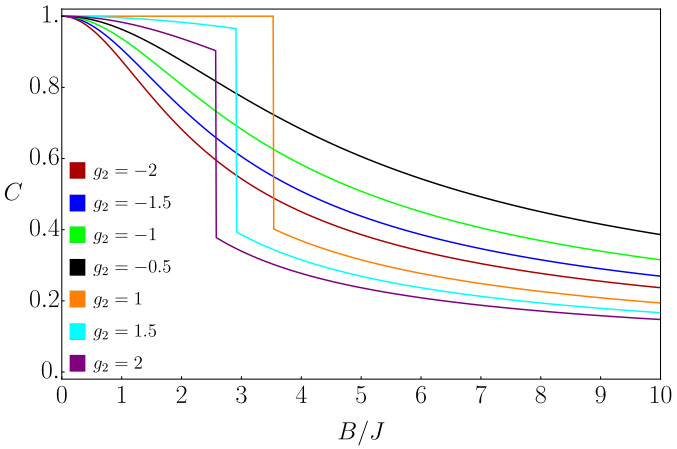

(a) $\Delta = 0.5$, $D = 0.1$, $J = 5$, $g_1 = 1$, $\gamma = 0.5$.

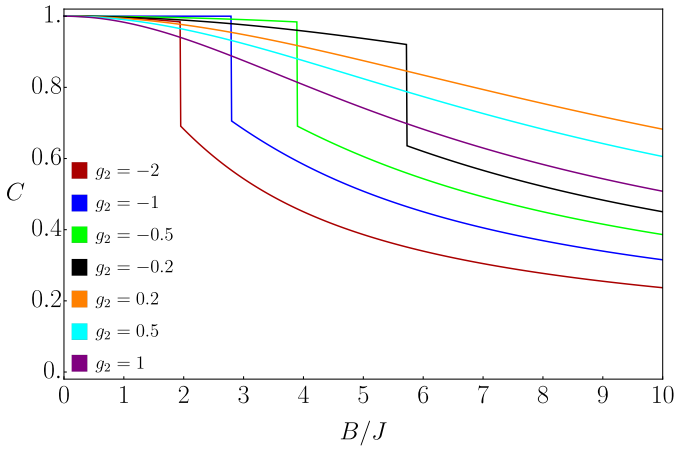

(b) $\Delta = 0.5$, $D = 0.1$, $J = 5$, $g_1 = 1$, $\gamma = 2$.

Figure 1: The dependence of concurrence on the magnetic field

Note that the states $\Psi_{3,4}$ have the form $|-\frac{1}{2},1\rangle \mp |\frac{1}{2},0\rangle$ under the condition $g_- = \frac{2D-J\Delta}{2B}$, and the states $\Psi_{5,6} = |\frac{1}{2},-1\rangle \mp |-\frac{1}{2},0\rangle$ at $g_- = \frac{J\Delta-2D}{2B}$, maximally entangled states.

Let us consider the dependence of entanglement(negativity, Ne) on several values of g_2 and the magnetic field at fixed values of the remaining parameters of the system. Let's fix the other parameters of the system as $\Delta = 0.8$, $D = 0.3$, $g_1 = 1$, $J = 3$. (Fig.2a)

In this case, for negative g_2 , the system is in the state Ψ_6 . For positive g_2 , we have a transition $\Psi_4 \mapsto \Psi_1$. The maximum value of entanglement for $\Psi_{4,6}$ for given parameters corresponds to the condition $g_2 = 1 \mp \frac{0.9}{B}$ respectively.

In Fig. 2b at $g_2 < -2.2$ we have transitions $\Psi_6 \mapsto \Psi_2 \mapsto \Psi_6$. When $-2.2 < g_2 < 0$, the system is in the state Ψ_6. For positive g_2, the transition $\Psi_4 \mapsto \Psi_1$ occurs. The maximum entanglement value for $\Psi_{4,6}$ for given parameters is achieved at $g_2 = 1 \pm \frac{2.3}{B}$, respectively. With the given parameters, it is possible to control the system using a magnetic field and achieve the maximum entanglement value at the field $B = \pm\frac{J\Delta-2D}{2g_-}$ for the states $\Psi_{4,6}$, respectively.

In **Chapter 2** a mixed spin trimer with two spin-1/2 and one spin-1 magnetic ions, with two different exchange couplings and two different but isotropic Landé g-factors was considered. We consider the case when an ion with spin 1 and one of the ions with spin 1/2 have g-factor equal to g_1

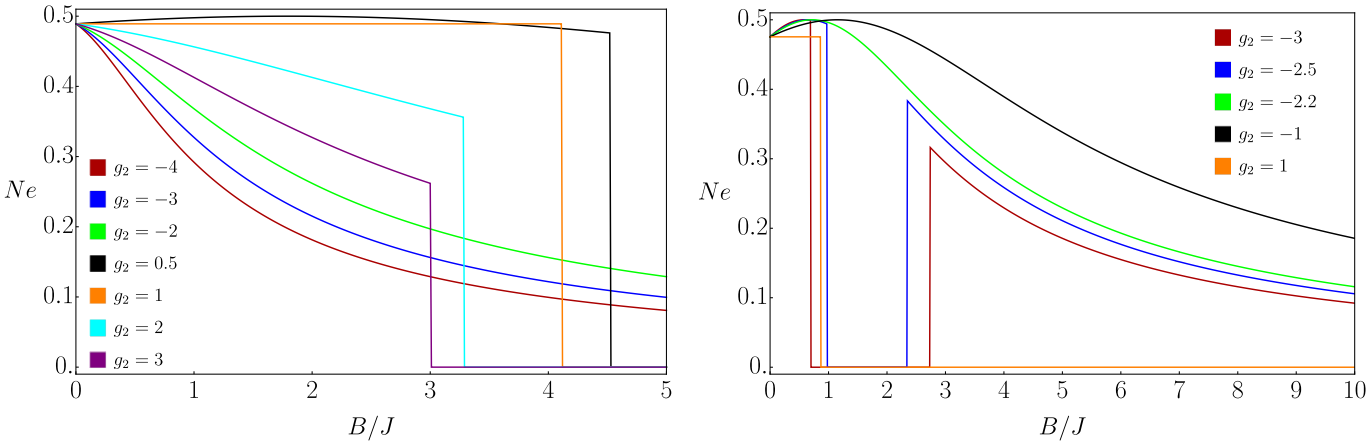

(a) $\Delta = 0.8$, $D = 0.3$, $g_1 = 1$, $J = 3$.

(b) $\Delta = 0.8$, $D = 0.3$, $g_1 = 1$, $J = -5$.

Figure 2: The dependence of negativity on the magnetic field

while the second spin-1/2 ion has g_2. Also, the distribution of exchange couplings is a bit unusual, as we assume that one of the ions with spin-1/2 interacts with spin-1 and another spin-1/2 with the same exchange constant, J_1. The main reason for such configuration of the system is its highest possible symmetry, facilitating the analytical finding of the Hamiltonian eigenvalues and eigenstates. For all quantities of interest analytical consideration is possible. The main focus is on how non-conserving magnetization affects quantum and thermal entanglement. Our main finding is that inhomogeneous g-factors for appropriate values of other parameters lead to enhancement of entanglement with respect to the case when all spins are taken to have the same g-factors.

The Hamiltonian of the model has the following form:

$$\mathscr{H} = J_1 \left(\boldsymbol{s}_1\boldsymbol{s}_2 + \boldsymbol{s}_2\boldsymbol{S}_3\right) + J_2\boldsymbol{s}_1\boldsymbol{S}_3 - B\left(g_1 s_1^z + g_2 s_2^z + g_1 S_3^z\right) \tag{5}$$

where $\boldsymbol{s}_a$, $a = 1,2$, are spin-1/2 operators, and $\boldsymbol{S}_3$ stands for spin-1 operators. The exchange interaction between all pairs of spins is supposed to be isotropic. Due to the presence of magnetic ions with two different g-factors, the magnetization operator does not commute with the Hamiltonian,

$$[\mathscr{H}, M^z] = iJ_1 g_- \left(s_1^x s_2^y - s_1^y s_2^x + s_2^y S_3^x - s_2^x S_3^y\right), \quad M^z = g_1 s_1^z + g_2 s_2^z + g_1 S_3^z, \quad g_- = g_1 - g_2. \tag{6}$$

However, $S_{tot}^z = s_1^z + s_2^z + S_3^z$ conserves. The Hamiltonian (5) of the system is diagonalized analyti-

cally. Detailed analysis of the ground state properties, revealing several possible ground state phase diagrams and magnetization profiles are presented. As the model under consideration has many parameters and possesses a non-conserving magnetization operator, the variety of possible ground state phase diagrams is quite large.

Without loss of generality one can consider five different types of ground state phase diagrams, given by the following conditions for the coupling constants: purely ferromagnetic, $J_1 = -1$, $J_2 \leq 0$; purely antiferromagnetic with equal couplings, $J_1 = J_2 = 1$; purely antiferromagnetic with non-equal couplings, $J_2 > 0, J_1 > 0$; two cases of mixed coupling, $J_1 = 1$, $J_2 \leq 0$ and $J_1 < 0$, $J_2 = 1$. Some eigenvectors did not change continuously under the conditions $g_1 \to g_2$ and $J_1 \to J_2$. In the case where $g_1 = g_2$ and $J_1 = J_2$, the corresponding eigenvectors are denoted as $|\psi_n\rangle_0$. We have

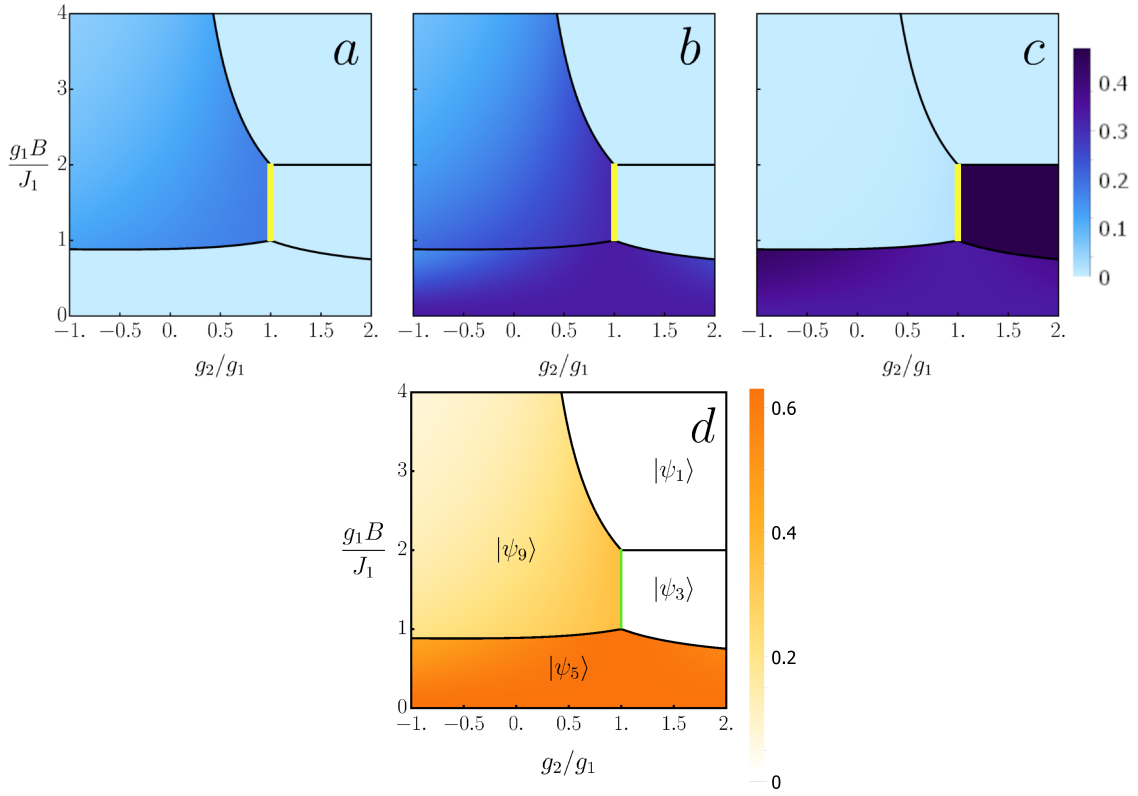

Figure 3: Density plots of negativity for the case of $J_1 = J_2 > 0$. Panels (a), (b) and (c) show the values of Ne_{12}, Ne_{23} and Ne_{13} respectively.

obtained analytic expressions for the bipartite and tripartite negativity for the eigenstates of the system under consideration. To demonstrate the overall picture of how quantum entanglement

changes across the various eigenstates, we present density plots of bipartite and tripartite negativity projected into the ground-state phase diagrams (Fig.3).

The most efficiently non-conserving magnetization affects the entanglement of the system spins in case of uniform antiferromagnetic couplings, $J_1 = J_2 > 0$. Possible ground states of the model are $|\psi_1\rangle, |\psi_3\rangle, |\psi_5\rangle$ and $|\psi_9\rangle$. However, at uniform g-factors, $g_2 = g_1$, $|\psi_3\rangle$ and $|\psi_9\rangle$ transform into $|\psi_3\rangle_0$ and $|\psi_9\rangle_0$. This fact is indicated in Fig. 3 by the yellow(in panels a,b,c) and green(in panel d) lines separating $|\psi_3\rangle$ and $|\psi_9\rangle$ at $g_2 = g_1$. It is obviously seen from density plots of the negativity, that systems with $g_2 \neq g_1$ exhibit much higher entanglement than their uniform counterpart, which is manifested in the most straightforward way for Ne_{13} within the $|\psi_3\rangle$ eigenstate. Magnetic field behaviour of negativity for both uniform and non-uniform g-factors cases is presented in Fig. 4.

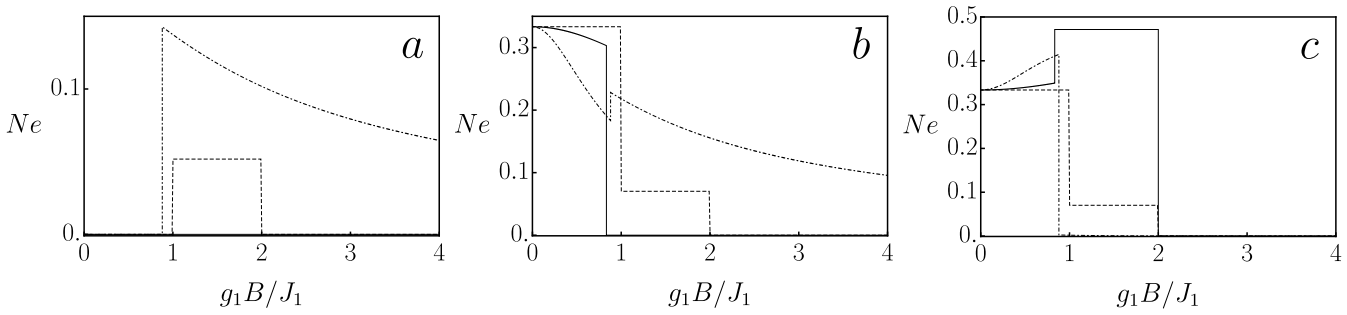

Figure 4: Negativity magnetic field dependence for the case $J_1 = J_2 > 0$. Panels (a), (b) and (c) show Ne_{12}, Ne_{23} and Ne_{13} respectively. In each panel solid line corresponds to $g_2 = 3/2$, dashed line corresponds to uniform-g case, $g_2 = g_1$, and dot-dashed line represent $g_2 = -1/2$ case.

The most significant enhancement of entanglement due to non-uniform g-factors occurs for the first and the third particles (panel (c)). The negativity curve for uniform g-factors has the same form as Ne_{23}, two plateaus at $1/3$ and $\frac{1}{16}\left(\sqrt{17}-3\right) \simeq 0.07$ corresponding to $|\psi_5\rangle$ and degenerate superposition of $|\psi_3\rangle_0$ and $|\psi_9\rangle_0$ respectively. Negativity curve for $g_2 = 3/2$ (solid) has weak magnetic field dependence within the $|\psi_5\rangle$ eigenstate where it demonstrates slow growth starting from $1/3$ value, but transition to the $|\psi_5\rangle$ eigenstate is accompanied with a jump to a constant value $Ne^5_{13} = \sqrt{3}/2 \simeq 0.47$ which is very close to maximal possible value, $1/2$. This is the highest value of negativity which can be achieved for the system under consideration. For the system with uniform antiferromagnetic exchange couplings, $J_1 = J_2 > 0$, even an arbitrary small difference between g_2

and g_1 brings to essential increase of negativity Ne_{13}. At finite temperatures, this high degree of quantum entanglement is maintained almost until $T/J = 0.2$, before it begins to fade away while remaining quite significant until $T/J = 0.2$. After this, with a subsequent increase in temperature, the negativity for a given pair of particles decreases to the level observed in the homogeneous case at zero temperature, $\frac{1}{16}(\sqrt{17}-3)$. Interestingly, the $|\psi_5\rangle$ eigenstate, which is the zero-field ground state for arbitrary value of g_2/g_1, exhibits maximal three-particle entanglement at $B = 0$ and at the segment $g_2 = g_1$, $Ne^5_{ABC} = \sqrt[3]{\frac{1}{4}} \approx 0.63$. Tripartite negativity is zero for $|\psi_3\rangle$, which means that this state is biseparable. Thus, in the case of $g_2 > g_1$, when magnetization is not conserved, it is possible to create three significantly different entanglement regimes (fully separable, biseparable, tripartite entangled) and control them by magnetic field.

In **Chapter 3**, key quantum characteristics of the mixed spin-(1/2,1,1/2) Heisenberg trimer under the influence of an external magnetic field have investigated. Specifically, we analyze the distributions of bipartite and tripartite entanglement quantified through the respective negativities, and the l_1-norm of coherence with the help of rigorous analytical and numerical methods. Our findings suggest that the heterotrinuclear molecular nanomagnet $[\{Cu^{II}L\}_2Ni^{II}(H_2O)_2](ClO_4)_2.3H_2O$, which represents an experimental realization of the mixed spin-(1/2,1,1/2) Heisenberg trimer, exhibits a significant bipartite entanglement between Cu^{II} and Ni^{II} magnetic ions along with robust tripartite entanglement among all three constituent $Cu^{II}Ni^{II}Cu^{II}$ magnetic ions. The significant bipartite and tripartite entanglement persists even at relatively high temperatures up to $37\,\mathrm{K}$ and magnetic fields up to $46\,\mathrm{T}$, whereby the coherence is maintained even at elevated temperatures. It is evidenced that the aforementioned molecular complex with the magnetic core $Cu^{II}Ni^{II}Cu^{II}$ provides an intriguing quantum resource, which exhibits a star-shaped state within the singlet eigenstate at low magnetic fields and W-like state within the triplet eigenstate at moderate magnetic fields. The model can be described by the following Hamiltonian:

$$\hat{H} = J\big(\hat{\boldsymbol{s}}_{\mathrm{a}}\cdot\hat{\boldsymbol{S}}_{\mathrm{b}} + \hat{\boldsymbol{S}}_{\mathrm{b}}\cdot\hat{\boldsymbol{s}}_{\mathrm{c}}\big) + D\big(\hat{S}^z_{\mathrm{b}}\big)^2 - g\mu_{\mathrm{B}}B\big(\hat{s}^z_{\mathrm{a}} + \hat{S}^z_{\mathrm{b}} + \hat{s}^z_{\mathrm{c}}\big). \tag{7}$$

Here, the first term of the Hamiltonian (7) expresses the nearest-neighbor exchange interactions between the spin operators $\hat{\boldsymbol{s}}_{\mathrm{a}}$ and $\hat{\boldsymbol{s}}_{\mathrm{c}}$ assigned to Cu^{II} ions and the spin operator $\hat{\boldsymbol{S}}_{\mathrm{b}}$ assigned to

the Ni^{II} ion respectively, with the antiferromagnetic coupling constant $J > 0$. The second term, D, refers to the single-ion anisotropy of the Ni^{II} ion. Finally, the last term is a standard Zeeman term, where g and B represent the Landé g-factor and the static magnetic field for the z-axis and μ_B is the Bohr magneton. The Hamiltonian (7) can be solved analytically through the exact diagonalization method and a full set of eigenvalues and eigenvectors can be obtained.

To provide a clear understanding of the thermal behavior of the mixed spin-(1/2,1,1/2) Heisenberg trimer, the density plot of tripartite as well as bipartite negativities are depicted in Fig. 5(a)-(c) for the particular case with the fixed value of the uniaxial single-ion anisotropy $D/J = 0.05$. The selection of a relatively weak easy-plane single-ion anisotropy for the results presented in Fig. 5 and all subsequent figures is inspired by previous experimental findings for the compound $Cu^{II}Ni^{II}Cu^{II}$.

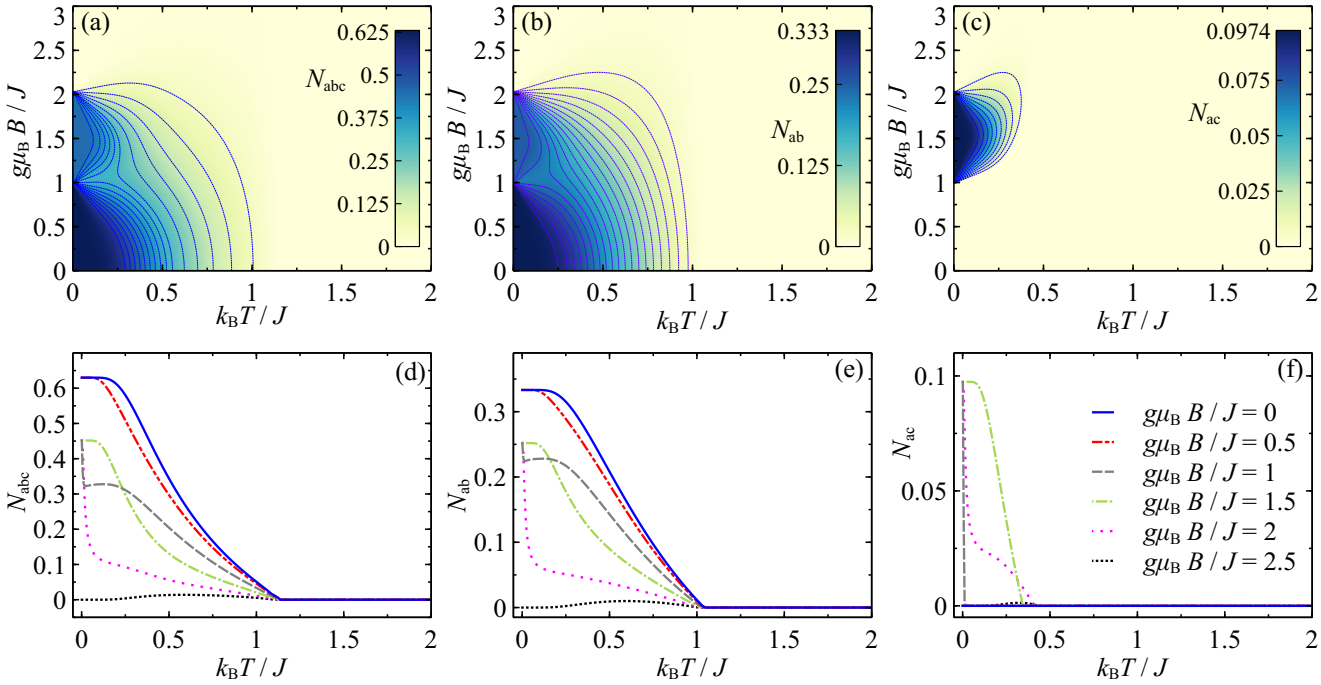

Figure 5: (a) The tripartite negativity N_{abc}, (b) the bipartite negativity N_{ab}, and (c) the bipartite negativity N_{ac} of the mixed spin-(1/2,1,1/2) Heisenberg trimer in the $g\mu_B B/J - k_B T/J$ plane by assuming $D/J = 0.05$; (d) Temperature dependencies of the N_{abc}, (e) N_{ab} and (f) N_{ac} for a few selected values of the magnetic field and $D/J = 0.05$.

It can be inferred from Figs. 5(b) and 5(c) that the bipartite negativities N_{ab} and N_{ac} form at low

enough temperatures plateaus quite similarly as the tripartite negativity N_{abc} does. The tripartite negativity N_{abc} and the bipartite negativity N_{ab} display their highest achievable values, $N_{\mathrm{abc}} = 0.625$ and $N_{\mathrm{ab}} = 1/3$, in a low-field region inherent to the singlet ground state $|\psi_9\rangle$, whereas the maximum of bipartite negativity $N_{\mathrm{ac}} \approx 0.0974$ can be found at moderate magnetic fields supporting the triplet ground state $|\psi_5\rangle$. Generally, the maximum values of both bipartite negativities are restricted to between 0 and 0.5. The absence of a direct exchange interaction between the outer spins s_{a} and s_{c} generally results in a lower value of the bipartite entanglement N_{ac} compared to the N_{ab} one assigned to directly interacting central and outer spins. A gradual vanishing of tripartite and bipartite negativities is observed along the temperature axis in all three density plots shown in upper panel.

The bottom panel in Fig. 5 demonstrates typical temperature dependencies of the tripartite and bipartite negativities N_{abc}, N_{ab} and N_{ac} for a few selected values of the magnetic field. A common property of all temperature dependencies of tripartite and bipartite negativities in Fig. 5(d)-(f) is the gradual thermally-induced decline in the tripartite and bipartite entanglement. In Fig. 5(d) the tripartite negativity starts from its highest value $N_{\mathrm{abc}} = 0.625$ achieved at zero magnetic field and vanishes at $k_{\mathrm{B}}T/J \approx 1.15$. As the magnetic field strengthens, the initial value of the tripartite negativity gradually decreases, while the threshold temperature at which it becomes zero remains unchanged. Contrary to this, the negativity N_{ac} measuring the bipartite entanglement between the outer spins is zero at low magnetic fields, but starts from the initial value $N_{\mathrm{ac}} \approx 0.0974$ at moderate magnetic fields $g\mu_{\mathrm{B}}B/J \gtrsim 1$ and is rapidly suppressed upon increasing temperature terminating at the threshold temperature $k_{\mathrm{B}}T/J \approx 0.4$ [see Fig. 5(f)]. The bipartite negativity N_{ab} follows trends similar to those of the tripartite negativity N_{abc} when reaching a maximum initial value $N_{\mathrm{ab}} = 1/3$ and vanishing at the same threshold temperature $k_{\mathrm{B}}T/J \approx 1.1$ [see Fig. 5(e)]. A less pronounced reentrance in the tripartite and bipartite entanglement can be found at magnetic fields slightly exceeding the saturation value $g\mu_{\mathrm{B}}B/J \gtrsim 2.5$ due to thermal excitations towards higher-energy levels. Besides, the peculiar changes in tripartite and bipartite entanglement observable around the magnetic fields $g\mu_{\mathrm{B}}B/J \approx 1$ and 2 can be again attributed to the relevant magnetic-field-driven phase transitions. Bearing all this in mind, we may proceed to a systematic classification of the quantum entanglement observed in the heterotrinuclear molecular complex $\mathrm{Cu^{II}Ni^{II}Cu^{II}}$. By considering specific values

of the coupling constant $J = 22.8\,\mathrm{cm}^{-1}$ and the uniaxial single-ion anisotropy $D = 0.05\,\mathrm{cm}^{-1}$, two distinct types of the quantum entanglement are identified in the molecular nanomagnet $\mathrm{Cu^{II}Ni^{II}Cu^{II}}$.

(I) **Star-shaped singlet state $|\psi_9\rangle$ (subtype 2-2):** At sufficiently low magnetic fields $B \lesssim 22.8\,\mathrm{T}$, the nonzero tripartite negativity N_{abc} quantifying entanglement among all three constituent $\mathrm{Cu^{II}Ni^{II}Cu^{II}}$ magnetic ions is accompanied with nonzero bipartite negativity $N_{\mathrm{ab}} = N_{\mathrm{bc}}$ between $\mathrm{Cu^{II}}$ and $\mathrm{Ni^{II}}$ magnetic ions, whereas the bipartite negativity N_{ac} between the two outer $\mathrm{Cu^{II}}$ magnetic ions is zero. The corresponding singlet ground state $|\psi_9\rangle$ thus belongs to the category of *star-shaped* states.

(II) **W-like triplet state $|\psi_5\rangle$ (subtype 2-3):** At moderate values of the magnetic field $22.8\,\mathrm{T} \lesssim B \lesssim 45.6\,\mathrm{T}$, all entanglement measures including the tripartite negativity N_{abc} and the bipartite negativities N_{ab}, N_{bc}, and N_{ac} become nonzero indicating the quantum entanglement between all three constituent $\mathrm{Cu^{II}Ni^{II}Cu^{II}}$ magnetic ions. The corresponding triplet ground state $|\psi_5\rangle$ can be accordingly categorized to *W-like* states.

In addition, it is worthwhile to remark that the thermal state emergent in a rather narrow range of temperatures $34\,\mathrm{K} \lesssim T \lesssim 37\,\mathrm{K}$, where the tripartite negativity is N_{abc} is nonzero even though all bipartite negativities N_{ab}, N_{bc}, and N_{ac} vanish, has signatures *GHZ-like* states (subtype 2-0).

CONCLUSIONS

1. In the case of a mixed spin-(1/2,1) system, the effect of any given parameters of the system can be compensated by magnetic field, and thus the maximal possible entanglement for the system can be obtained. In the considered two-particle systems, in the case of an antiferromagnet, increasing the magnetic field leads to the transition into a state with less entanglement for both systems. For ferromagnets with a positive g_1 there are a negative values of g_2, at which the system gets into a state with greater entanglement.

2. A model of a triangular mixed spin-(1/2, 1/2, 1) molecular magnet was studied. For all ground states of the system analytical expressions for bipartite and tripartite entanglement were found. In the case of homogeneous antiferromagnetic exchange interaction, three entanglement regimes controllable by a magnetic field was obtained: fully separable(the system is not entangled), almost maximally entangled biseparable(only one pair is entangled), maximally tripartite entangled (all three particles are entangled). The biseparable intermediate regime is possibly only in the case of non-conserved magnetization (inhomogeneous Lande factors).

3. Molecular magnets with non-conserved magnetization provide a more efficient means of manipulating quantum entanglement through magnetic fields. A key distinction from the uniform g-case is the ability to have a continuous dependency of negativity on the magnetic field within the same ground state, as well as the potential to achieve highly entangled eigenstates.

4. We also investigated the mixed spin-(1/2,1,1/2) Heisenberg trimer in external magnetic fields, designed for theoretical modeling of molecular nanomagnets such as $Cu^{2+}Ni^{2+}Cu^{2+}$. Through extensive analytical and numerical calculations, we analyzed the distributions of bipartite and tripartite entanglement, as well as the l_1-norm of quantum coherence. The system exhibits significant entanglement even at relatively high temperatures and magnetic fields. The molecular compound $\mathrm{Cu}^{2+}\mathrm{Ni}^{2+}\mathrm{Cu}^{2+}$ exhibits star-shaped entanglement in weak magnetic fields and W-shaped entanglement in fairly strong magnetic fields. In addition, the work predicts that the molecular nanomagnet should exhibit a high degree of quantum coherence that is maintained even at high temperatures, despite significant thermal fluctuations.

PUBLICATIONS ON THE TOPIC OF THE THESIS

1. Z. A. Adamyan, S. A. Muradyan, and V. R. Ohanyan. "Quantum entanglement in spin dimers: effects of a magnetic field and heterogeneous g-factors." Journal of Contemporary Physics (Armenian Academy of Sciences) **55** (2020): 292-298.

2. Zhirayr Adamyan, and Vadim Ohanyan. "Quantum entanglement in a mixed-spin trimer: Effects of a magnetic field and heterogeneous g factors." Physical Review E **110.3** (2024): 034131.

3. Zh. A. Adamyan "Quantum Entanglement in a Mixed Spin Trimer (1/2, 1/2, 1) with Non-Conserved Magnetization at Finite Temperatures." Journal of Contemporary Physics (Armenian Academy of Sciences) **59.3** (2024): 279-286.

4. Azadeh Ghannadan, Hamid Arian Zad, Saeed Haddadi, Jozef Strečka, Zhirayr Adamyan, and Vadim Ohanyan. "Molecular nanomagnet $Cu^{2+}Ni^{2+}Cu^{2+}$ as a resource for bipartite and tripartite quantum entanglement and coherence." Physical Review A **111**, no. 2 (2025): 022605.

ԱՄՓՈՓԱԳԻՐ

Ատենախոսությունում հետազոտված են սպինային դիմերների և տրիմերների խճճվածության հատկությունները: Հիմնական արդյունքները ներառում են օպտիմալ խճճվածություն ստեղծելու պայմանների ուսումնասիրումը, չպահպանվող մագնիսացվածության էֆեկտների հետազոտումը, մագնիսական դաշտերի և ջերմաստիճանի օգտագործմամբ քվանտային խճճվածության կառավարման հնարավորության ցուցադրումը: Այս արդյունքները նպաստում են քվանտային տեխնոլոգիաների զարգացմանը՝ օգտագործելով մոլեկուլային մագնիսները (SMMs) որպես կառուցվածքային բլոկներ:

1. Ցույց է տրվել, որ խառը սպին (1/2,1) համակարգի դեպքում ցանկացած պարամետրի ազդեցությունը կարող է կոմպենսացվել մագնիսական դաշտով և այդպիսով հնարավորություն տալով ձեռք բերել համակարգի համար առավելագույն խճճվածություն: Դիտարկված երկմասնիկանի համակարգերում անտիֆերոմագնիսական փոխազդեցության դեպքում մագնիսական դաշտի մեծացման ժամանակ երկու համակարգերն էլ քվանտային փուլային անցում են կատարում ավելի փոքր խճճվածությամբ վիճակների: Իսկ ֆերոմագնիսական փոխազդեցության դեպքում, երբ մասնիկների g_1 և g_2 Լանդեի ֆակտորներն ունեն հակառակ նշաններ, համակարգը փուլային անցում է կատարում ավելի մեծ խճճվածությամբ վիճակի:

2. Ուսումնասիրվել է եռանկյունաձև խառը սպին (1/2, 1/2, 1) մոլեկուլային մագնիսի մոդելը: Համակարգի բոլոր հիմնական վիճակների համար ստացվել են երկմասնիկ և եռամասնիկ խճճվածության անալիտիկ տեսքերը: Համասեռ անտիֆերոմագնիսական փոխանակային փոխազդեցության դեպքում ստացվել է մագնիսական դաշտով կառավարվող երեք խճճվածության ռեժիմներ՝ ամբողջովին անջատելի (համակարգը խճճված չէ), գրեթե մաքսիմալ խճճված երկանջատելի (միայն մեկ զույգը խճճված), մաքսիմալ եռամասնիկ խճճված (բոլոր երեք մասնիկները խճճված են): Երկանջատելի միջանկյալ ռեժիմն ի հայտ է գալիս բացառապես չպահպանվող մագնիսացվածության դեպքում (անհամասեռ Լանդեի գործակիցներ):

3. Աշխատանքում ցույց է տրվել, որ խճճվածության կառավարումը մագնիսական դաշտերի

միջոցով ավելի արդյունավետ է չպահպանվող մագնիսացվածությամբ մագնիսական մոլեկուլներում: Համասեռ Լանդեի գործակիցների դեպքի համեմատ հիմնական տարբերությունն այն է, որ խճճվածությունը նույն հիմնական վիճակում ունի անընդհատ կախվածություն մագնիսական դաշտից: Բացի այդ, անհամասեռ Լանդեի գործակիցներով մոդելները նոր հնարավորություններ են ստեղծում ուժեղ խճճված սեփական վիճակների ստացման համար:

4. Ուսումնասիրվել է խառը սպին (1/2,1,1/2) եռամասնիկ համակարգը արտաքին մագնիսական դաշտում, որը նախատեսված է մոլեկուլային նանոմագնիսների (օրինակ՝ $Cu^{2+}Ni^{2+}Cu^{2+}$) տեսական մոդելավորման համար: Անալիտիկ և թվային հաշվարկների միջոցով ուսումնասիրվել են երկմասնիկանի և եռամասնիկանի խճճվածության բաշխումները, ինչպես նաև քվանտային կոհերենտության l_1-նորմը: Ցույց է տրվել, որ նշված համակարգը ցուցաբերում է զգալի խճճվածություն անգամ համեմատաբար բարձր ջերմաստիճանների և մագնիսական դաշտերի դեպքում: $Cu^{2+}Ni^{2+}Cu^{2+}$ մոլեկուլային միացությունը ցածր մագնիսական դաշտերում ցուցաբերում է աստղաձև վիճակի խճճվածություն, իսկ բավականաչափ ուժեղ մագնիսական դաշտերում W-ձև վիճակի եռամասնիկ խճճվածություն: Բացի այդ, աշխատանքում կանխատեսվում է, որ մոլեկուլային նանոմագնիսը պետք է դրսևորի քվանտային կոհերենտության բարձր աստիճան, որը պահպանվում է նույնիսկ բարձր ջերմաստիճաններում՝ չնայած զգալի ջերմային տատանումներին:

Адамян Жирайр

Некоторые задачи низкоразмерного квантового магнетизма

В данной диссертационной работе представлен тщательный анализ свойств квантовой запутанности низкоразмерных квантовых систем, некоторых моделей молекулярных магнитов. В частности, в работе изучены свойств запутанности спиновых димеров и тримеров. Основные выводы диссертации касаются определения физических условий, которые соответствуют оптимальному запутыванию, исследования эффектов несохраняющейся намагниченности и демонстрации потенциала манипулирования квантовыми состояниями с использованием магнитных полей и температуры. Эти результаты способствуют лучшему пониманию фундаментальных

основ и потенциальной разработке квантовых технологий, использующих молекулярные магниты (SMM) в качестве носителей квантовых состояний (кубитов, кутритов и т.д.).

1. Было показано, что в случае спинового димера со смешанными спинами-(1/2,1) воздействие любых заданных параметров системы можно компенсировать некоторым магнитным полем и, таким образом, получить максимальное возможное для системы значение запутанности. В наблюдаемых двухчастичных системах в случае антиферромагнитных взаимодействий при повышении значения магнитного поля обе системы переходят в состояние с меньшей запутанностью. Для ферромагнитных взаимодействий при положительном g_1 существуют некоторые отрицательные значения g_2 , при которых система переходит в состояние с большей запутанностью.

2. Рассмотрена модель треугольного спинового тримера со смешанными спинами (1/2, 1/2, 1). Для всех основных состояний системы были получены аналитические выражения для двухчастичной и трехчастичной запутанности. В случае однородного антиферромагнитного обменного взаимодействия было показано, что в процессе намагничивания (размагничивания) система последовательно проходит через основные состояния с тремя различными режимами квантовой запутанности: сепарабельное состояние (система не запутана), почти максимально запутанная бисепарабельное состояние (запутанна одна пара) и максимально трехчастичная запутанное состояние (все три частицы запутаны). При этом промежутаное бисепарабельное состояние возникают исключительно в случае несохраняющейся намагниченности (неоднородных множителей Ланде).

3. В работе показанно, что эффективное управление запутанностью с помощью магнитных полей может быть реализовано в магнитных молекулах с несохраняющейся намагниченностью. Главное отличие по сравнению со случаем однородных множителей Ланде заключается в том, что запутанность в пределах одного и того же основного состояния имеет непрерывную зависимость от магнитного поля. Кроме того, модели с неоднородными множителями Ланде создают новые возможности для получения сильно запутанных собственных состояний.

4. Рассмотрена модель спинового тримера со смешанными спинами, (1/2,1,1/2) в линейной геометрии, которая является теоретической моделью некоторых молекулярных наномагнетиков (например, $Cu^{2+}Ni^{2+}Cu^{2+}$). Аналитические и численные расчеты были использованы для изучения распределений двухчастичной и трехчастичной запутанности, а также l_1-нормы квантовой когерентности. Было показано, что рассматриваемая система демонстрирует значительную запутанность даже при относительно высоких температурах и магнитных полях. Молекулярное соединение $Cu^{2+}Ni^{2+}Cu^{2+}$ демонстрирует звездообразную запутанность в слабых магнитных полях и W-образную запутанность в достаточно сильных магнитных полях. Кроме того, работа предсказывает, что молекулярный наномагнит должен демонстрировать высокую степень квантовой когерентности, которая сохраняется даже при высоких температурах, несмотря на значительные тепловые флуктуации.